

METAL ABUNDANCE PROPERTIES OF M81 GLOBULAR CLUSTER SYSTEM

JUN MA¹, DAVID BURSTEIN², ZHOU FAN^{1,3}, XU ZHOU¹, JIANGSHENG CHEN¹, ZHAOJI JIANG¹, ZHENYU WU¹ AND JIANGHUA WU¹

PASP, in press

ABSTRACT

This paper is the third in the series of papers on M81 globular clusters. In this paper, we present spatial and metal abundance properties of 95 M81 globular clusters, which comprise nearly half of all the M81 globular cluster system. These globular clusters are divided into two M81 metallicity groups by a KMM test. Our results show that, the metal-rich clusters did not demonstrate a centrally concentrated spatial distribution as ones in M31, and metal-poor clusters tend to be less spatially concentrated. In other words, the distribution of the metal-rich clusters in M81 is not very similar to that of M31. Most of the metal-rich clusters distribute at projected radii of 4-8 kpc. It is also noted that the metal-rich clusters distribute within the inner 20 kpc, and the metal-poor ones do out to radii of ~ 40 kpc. Like our Galaxy and M31, the metallicity distribution of globular clusters in M81 along galactocentric radius suggests that some dissipation occurred during the formation of the globular cluster system, i.e. smooth, pressure-supported collapse models of galaxies are unlikely to produce such radial distribution of metallicity presented in this paper. There is not evident correlation between globular cluster luminosity and metallicity in M81 globular clusters. The overwhelming conclusion of this paper seems to be that a more complete and thorough cluster search is needed in M81.

Subject headings: galaxies: individual (M81) – galaxies: star clusters – globular clusters: general

1. INTRODUCTION

An understanding of galaxy formation and evolution is one of the principal goals of modern astrophysics. Globular clusters are fossils of the earliest stages of galaxy formation and evolution. They are bright, easily recognized packages containing a stellar population with a homogeneous abundance and age. So, their integrated properties of location, abundance, and kinematics provide valuable clues to the nature and duration of galaxy formation (Barmby et al. 2000).

The metallicity distribution of globular clusters is of particular importance in deepening our knowledge of the dynamical and chemical evolution of the parent galaxies. For example, the globular clusters of many elliptical galaxies show multi-modal metallicity distributions, suggesting that multiple star formation episodes occurred in these elliptical galaxies in the past (Zepf & Ashman 1993; Barmby et al. 2000). Great progress has been made in the past decade in our understanding of globular cluster systems of galaxies, especially the discovery that many galaxies possess two or more distinct subpopulations of globular clusters (e.g., West et al. 2004, and references therein). Based on the data from *Hubble Space Telescope* (*HST*) archive, Gebhardt & Kissler-Patig (1999), Larsen et al. (2001) and Kundu & Whitmore (2001) presented that many large galaxies possess two or more subpopulations of globular clusters that have quite different chemical compositions. Recently, Peng et al. (2006) presented the color distributions of globular cluster systems for 100

early-type galaxies observed in the Virgo Cluster Survey with the Advanced Camera for Surveys (ACS) on the *HST*, and found that, on average, galaxies at all luminosities in their study appear to have bimodal or asymmetric GC color/metallicity distributions. The presence of color-bimodality indicates that there have been at least two major star-forming mechanisms in the histories of galaxies.

Côté (1999) presented a metallicity distribution of 133 Galactic globular clusters that apparently shows two peaks (i.e., two distinct metal-poor and metal-rich globular cluster populations). A double-Gaussian can best fit these two subpopulations, the mean metallicity values are -1.59 and -0.55 dex, respectively. Using the data for 247 globular clusters in M31, Barmby et al. (2000) studied the metallicity distribution, which is asymmetric, implying the possibility of bimodality. Then they applied a KMM algorithm showing that the metallicity distribution is really bimodal. Perrett et al. (2002) confirmed the conclusions of Barmby et al. (2000). Ma et al. (2005) showed that the intrinsic B and V colors and metallicities of 94 M81 globular clusters are bimodal, with metallicity peaks at $[\text{Fe}/\text{H}] \approx -1.45$ and -0.53 , similar to what we find for the Milky Way and M31 globular clusters.

M81 is one of the nearest Sa/Sb-type spiral outside the Local Group, very similar to M31, and roughly as massive as the Milky Way. So, beyond the Local Group, it is a good candidate for reaching a detailed study of spiral galaxy globular cluster system for comparison to the Milky Way and M31 system. Brodie & Huchra (1991) derived spectroscopic metallicities for eight globular clusters in M81 and presented the sample mean of $[\text{Fe}/\text{H}] = -1.46 \pm 0.31$. Perelmuter et al. (1995) obtained low signal-to-noise spectra of 82 candidates, 25 of which were confirmed as *bona fide* M81 globular clusters. They derived the mean metallicity to be $[\text{Fe}/\text{H}] = -1.48 \pm 0.19$

¹ National Astronomical Observatories, Chinese Academy of Sciences, Beijing, 100012, P. R. China, majun@vega.bac.pku.edu.cn

² Department of Physics and Astronomy, Box 871504, Arizona State University, Tempe, AZ 85287-1504

³ Graduate University of Chinese Academy of Sciences, 19A Yuquan Road, Shijingshan District, Beijing 100049, China

both from the weighted mean of the individual metallicities, and directly from the composite spectrum of the 25 confirmed globular clusters. To maximize the success rate of the globular cluster candidate list for the ongoing spectroscopic observations, Perelmuter & Racine (1995) used an extensive database that included photometric, astrometric, and morphological information on 3774 objects covering over a > 50 arcmin diameter field centered on M81 to reveal 70 globular cluster candidates.

Schroder et al. (2002) presented moderate-resolution spectroscopy for 16 globular cluster candidates from the list in Perelmuter & Racine (1995), and confirmed these 16 candidates as *bona fide* globular clusters. They also obtained metallicities for 15 of the 16 globular clusters. From their results, Schroder et al. (2002) concluded that the M81 globular cluster system is very similar to the Milky Way and M31 systems, both chemically and kinematically.

With the superior resolution of the *HST*, M81 is close enough for its clusters to be easily resolved on the basis of image structure (Chandar et al. 2001). Thus, using the *B*, *V*, and *I* bands of *HST* Wide Field Planetary Camera 2 (WFPC2), Chandar et al. (2001) imaged eight fields covering a total area of ~ 40 arcmin², and detected 114 compact star clusters in M81, 59 of which are globular clusters. Based on the estimated intrinsic colors, Chandar et al. (2004) found that the M81 globular cluster system has an extended metallicity distribution, which argues the presence of both metal-rich and metal-poor globular clusters. Ma et al. (2005) then confirmed this conclusion.

The outline of the paper is as follows. In § 2 we provide some statistical relationships. The summary is presented in § 3.

2. PROPERTIES OF GLOBULAR CLUSTERS IN M81

2.1. Sample of globular clusters

In the first paper of our series, Ma et al. (2005) studied the distributions of intrinsic *B* and *V* colors and metallicities of 95 M81 globular clusters which are from Perelmuter et al. (1995), Chandar et al. (2001) and Schroder et al. (2002). This cluster sample includes nearly half of the M81 total globular cluster population. About the M81 total globular cluster population, Perelmuter & Racine (1995) estimated it to be 210 ± 30 by the *BVR* photometric, astrometric, and image structure study of the M81 field; Chandar et al. (2001) indicated the total number of globular clusters in M81 to be 211 ± 29 using globular cluster estimates in various annular bins and correcting for incompleteness. It is difficult to detect and confirm globular clusters beyond the Local Group before *HST* appears. In fact, even in the Local Group, it is also not easy to detect and confirm globular clusters. For example, the total number of globular clusters in M31 was estimated to be 460 ± 70 by Barmby & Huchra (2001), the largest number of globular clusters used to study the metal abundance properties of the M31 globular clusters includes 301 clusters collected by Perrett et al. (2002), a little more than half of the total number. Beyond the Local Group, the globular cluster sample in M81 collected by Ma et al. (2005) includes the largest number of globular clusters comparing to the total globular clusters in the host galaxy.

FIG. 1.— The image of M81 in filter BATC07 (5785Å) and the positions of the sample star clusters. The center of the image is located at RA = 01^h33^m50^s.58 Dec=30°39′08″.4 (J2000.0). North is up and east is to the left.

In the second paper of our series, Ma et al. (2006) presented the spectral energy distributions of 42 M81 globular clusters selected from Ma et al. (2005) in 13 intermediate-band filters from 4000 to 10000Å, using the CCD images of M81 observed as part of the Beijing-Arizona-Taiwan-Connecticut (hereafter BATC) multicolor survey of the sky, and confirmed the conclusions of Schroder et al. (2002) that, M81 contains clusters as young as a few Gyrs, which were also observed in both M31 and M33. In this paper, we will study the spatial and metal abundance properties of the M81 globular clusters using the sample globular clusters of Ma et al. (2005). Figure 1 is the image of M81 in filter BATC07 (5785Å) of BATC multicolor survey of the sky, the circles indicate the positions of the sample clusters.

As mentioned above, Ma et al. (2005) studied the distributions of intrinsic *B* and *V* colors and metallicities of these 95 M81 globular clusters, and first found that the abundance distribution of the globular cluster system is consistent with a bimodal distribution with peaks at $[\text{Fe}/\text{H}] \approx -1.45$ and -0.53 based on the KMM algorithm of Ashman et al. (1994). It is true that, the appearance of the histogram can be ambiguous and misleading with binned data, however, the KMM algorithm of Ashman et al. (1994) is a robust method of analysis without relying on binning methods (see Perrett et al. 2002). KMM mixture modelling works under the assumption that the sample data are independently drawn from a parent population that comprises a mixture of *N* Gaussian distributions. Ma et al. (2005) presented that, for M81 globular clusters, the posteriori probabilities of group membership returned by the KMM algorithm assigned 74 clusters to the metal-poor population and 20 to the metal-rich population distribution⁴.

2.2. Spatial distribution

Figure 2 shows the projected spatial distributions of the metal-poor and metal-rich globular clusters in M81. The distance modulus for M81 is adopted to be 27.8 (Freedman et al. 1994; Chandar et al. 2001). We adopted the inclination and position angles to be 59° and 157° of M81 as Chandar et al. (2001) did, respectively. When the line of intersection (i.e. the major axis of the image) between the galactic plane and tangent plane is taken as the polar axis, it is easily proved that:

$$r = \rho \sqrt{1 + \tan^2 \gamma \sin^2 \theta} \quad (1)$$

and

$$\tan \phi = \frac{\tan \theta}{\cos \gamma}, \quad (2)$$

where *r* and ϕ are the polar co-ordinates in the galactic plane, and ρ and θ are the corresponding co-ordinates in the tangent plane, and γ is the inclination angle of

⁴ Since the globular cluster 96 of Chandar et al. (2001) has very high $(B-V)_0$ ($(B-V)_0 = 1.778$), and the metallicity obtained using the color-metallicity correlation is too rich (0.95 dex), Ma et al. (2005) do not include it when performing the KMM test.

the galactic disk. Using formula (1), we can obtain the distances of our sample clusters from the center of M81, which are listed in Table 1. In Table 1, we also listed the metallicities of the sample clusters from Ma et al. (2005). From Figure 2, it is clear that the metal-rich globular clusters in M81 are not as centrally concentrated as the metal-poor globular clusters of M31 are (Huchra et al. 1991; Perrett et al. 2002). Figure 3 presents the histogram for the metal-poor and metal-rich globular clusters in M81. It shows that most of the metal-rich clusters distribute at projected radii of 4-8 kpc. It is also noted that the metal-rich clusters distribute within the inner 20 kpc, and the metal-poor ones do out to radii of ~ 40 kpc. In the Milky Way, the metal-rich GCs reveal significant rotations and have historically been associated with the thick-disk system (Zinn 1985; Armandroff 1989); however, other works (Frenk & White 1982; Minniti 1995; Côté 1999; Forbes et al. 2001) suggested that metal-rich GCs within ~ 5 kpc of the Milky Way Galactic center are better associated with the bulge and bar. In M31, Elson & Waltherbos (1988) showed that the metal-rich clusters constitute a more highly flatted system than the metal-poor ones, and appear to have disklike kinematics; Huchra et al. (1991) showed that the metal-rich GCs are preferentially close to the galaxy center. At the same time, Huchra et al. (1991) showed that the distinction between the rotation of the metal-rich and metal-poor clusters is most apparent in the inner 2 kpc. So, Huchra et al. (1991) concluded that the rich-metal clusters in M31 appear to form a central rotating disk system. With the largest sample of 321 velocities, Perrett et al. (2002) provided a more comprehensive investigation on the kinematics of the M31 cluster system. Perrett et al. (2002) showed that, the metal-rich globular clusters of M31 appear to constitute a distinct kinematic subsystem that demonstrates a centrally spatial distribution with a high rotation amplitude, but does not appear significantly flattened, which is consistent with a bulge population. It is of interests to mention that, Schroder et al. (2002) performed a maximum-likelihood kinematic analysis on 166 M31 clusters of Barmby et al. (2000) and found that the most significant difference between the rotation of the metal-rich and metal-poor clusters occurs at intermediate projected galactocentric radii. Especially, Schroder et al. (2002) presented a potential thick-disk population among M31's metal-rich globular clusters. For M81 globular clusters, Schroder et al. (2002) performed a kinematic analysis of the velocities of 44 M81 globular clusters, and strongly suggested that the metal-rich clusters are rotating in the same sense as the gas in the disk of M81. Schroder et al. (2002) concluded that, although their cluster sample is not large enough to make a direct comparison between metal-rich and metal-poor clusters in specific radius ranges, the conclusion with M81's metal-rich clusters at intermediate projected radii being associated with a thick disk in M81 is correct. It is true that, from Figure 3, most of metal-rich clusters distribute at projected radii of 4-8 kpc. So, at least, we can conclude that most of the metal-rich clusters in our sample are not associated with a bulge cluster system of M81; they may associate with a thick disk in M81 as indicated by Schroder et al. (2002). The sample clusters of this paper include all the sample clusters of Schroder et al. (2002). But, except for the sample clus-

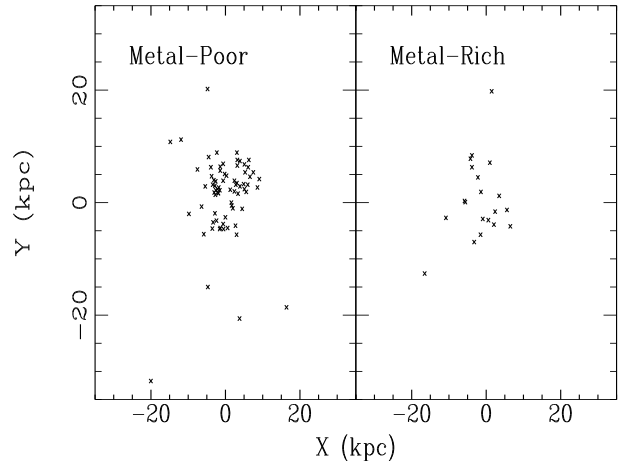


FIG. 2.— Spatial distributions of the metal-rich and metal-poor globular clusters.

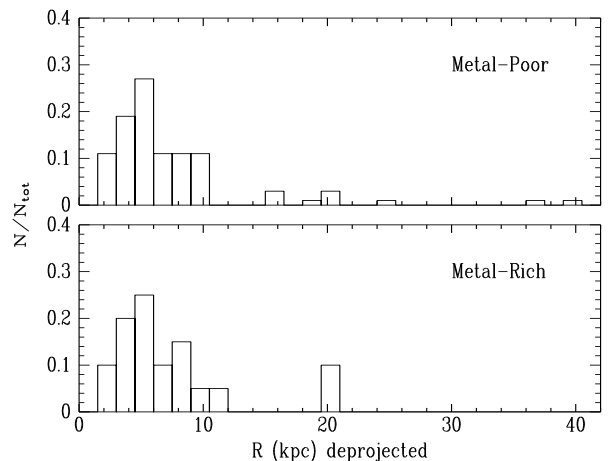


FIG. 3.— Radial distributions of the metal-rich and metal-poor globular clusters.

ters of Schroder et al. (2002), the other clusters have not published radial velocity estimates. So, obviously, more kinematic and metallicity data are needed for globular clusters in M81 to determine if the inner metal-rich GCs have kinematic properties that are consistent with the bulge and the metal-rich GCs at projected radii of 4-8 kpc are associated with a thick disk in M81.

2.3. Metallicity gradient

The presence or absence of a radial trend in globular cluster metallicities is an important test of galaxy formation theory (Barmby et al. 2000). If a galaxy forms as a consequence of a monolithic dissipative and rapid collapse of a single massive, nearly-spherical spinning gas cloud in which the enrichment timescale is shorter than the collapse time, the halo stars and globular clusters should show large-scale metallicity gradients (Eggen et al. 1962; Barmby et al. 2000); however, Searle & Zinn (1978) presented a chaotic scheme in the early evolution of a galaxy, in which loosely bound pre-enriched fragments merge with the main body of the proto-galaxy over a significant period, so there should

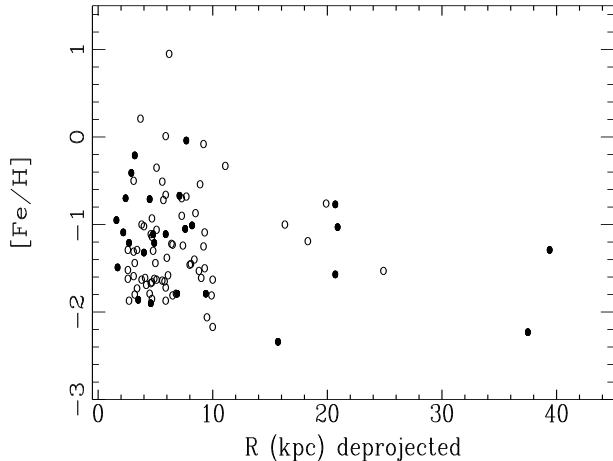


FIG. 4.— Metallicity as function of projected radius for M81 globular clusters. Black circles indicate the clusters with spectroscopic metallicities with uncertainties smaller than 1.0 dex.

be homogeneous metallicity distribution. For the Milky Way, Armandroff (1989) showed some evidence that metallicity gradients with both distance from the Galactic plane and distance from the Galactic center were present in the disk cluster system. For M31, there are some inconsistent conclusions, such as van den Bergh (1969) showed that there is little or no evidence for a correlation between metallicity and projected radius, but most of his clusters were inside $50'$; however, some authors (see e.g. Huchra et al. 1982; Sharov 1988; Huchra et al. 1991; Perrett et al. 2002) presented that there is evidence for a weak but measurable metallicity gradient as a function of projected radius. Barmby et al. (2000) confirmed the latter result based on their large sample of spectral metallicity and color-derived metallicity. Figure 4 plots the metallicity of the M81 globular clusters as a function of galactocentric radius, in which black circles indicate the clusters with spectroscopic metallicities with uncertainties smaller than 1.0 dex. Clearly, the dominant feature of this diagram is the scatter in metallicity at any radius. At the same time, our sample clusters are mainly distributed in the inner 10 kpc. So, it is difficult to determine the metallicity gradient. It is true that, smooth, pressure-supported collapse models of galaxies are unlikely to produce a result like this. However, in order to present a quantitative conclusion, we made least-squares fits: the total sample of globular clusters does not have a significant metallicity gradient (-0.009 ± 0.009 dex kpc^{-1}), and the clusters with spectroscopic metallicities with uncertainties smaller than 1.0 dex have a marginally significant gradient (-0.018 ± 0.01 dex kpc^{-1}). This result is in agreement with Kong et al. (2000), who obtained metallicity maps of M81 field by comparing simple stellar population synthesis models of BC96 (Bruzual & Charlot 1996) with the integrated photometric measurements of the BATC photometric system, and did not find, within their errors, any obvious metallicity gradient from the central region to the bulge and disk of M81. But, we should emphasize that, in the least-squares fits of this paper, the metal-rich clusters seem to act an important part in determining the metallicity gradient. From Figure 4, we can also see the decrease in the “upper envelope” of metallicity re-

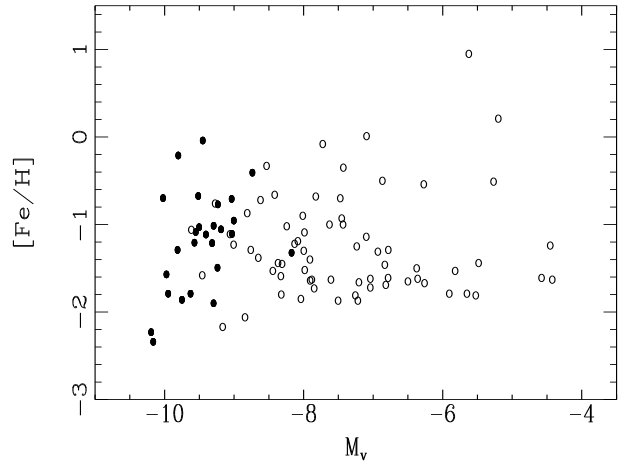


FIG. 5.— Metallicity versus absolute magnitude for M81 globular clusters. Black circles indicate the clusters with spectroscopic metallicities with uncertainties smaller than 1.0 dex.

ported by Huchra et al. (1991) and Barmby et al. (2000) for M31 globular clusters. In fact, we do a least-squares fits for the metal-poor clusters of M81, the metallicity gradient is -0.006 ± 0.006 dex kpc^{-1} . This metallicity gradient may not have any statistical meanings. It is clear that, the small sample of rich-metal clusters in M81 cannot present any firm conclusion about metallicity gradient.

2.4. Metallicity versus absolute magnitude

The correlation between cluster mass (or luminosity) and metallicity is important in globular cluster formation theory. It is generally believed that, if self-enrichment is important in globular clusters, the most massive clusters could retain their metal-enriched supernova ejecta, so the metal abundance should increase with cluster mass; the opposite is true if cooling from metals determines the temperature in the cluster-forming clouds (Barmby et al. 2000). The self-enrichment of GCs has been in detail studied in some aspects (see detail from Strader et al. 2006). However, it is interesting of mentioning the model of globular cluster self-enrichment developed by Parmentier et al. (1999). In this model, cold and dense clouds embedded in the hot protogalactic medium are assumed to be the progenitors of galactic halo globular clusters. Based on this model, Parmentier & Gilmore (2001) presented that the most metal-rich proto-globular clusters are the least massive ones.

For M31 globular clusters, Huchra et al. (1991) first presented the metallicity versus apparent magnitude for 150 M31 clusters, and did not find any trend of metallicity with luminosity; then, Barmby et al. (2000) showed metallicity versus dereddened apparent magnitude using a large cluster sample including 247 objects, and confirmed the conclusion of Huchra et al. (1991).

Figure 5 shows metallicity versus absolute magnitude for M81 globular clusters, in which black circles indicate the clusters with spectroscopic metallicities with uncertainties smaller than 1.0 dex. The metallicity and absolute magnitudes for the sample clusters are from Ma et al. (2005). It is true that there is not obvious trend of metallicity with luminosity as M31 GCs do. Least-squares fits show no evidence for a relationship between

luminosity and metallicity in M81 clusters.

As we know, *HST* provides a unique tool for studying globular clusters in extragalaxies. Recently, based on the ACS on the *HST*, Harris et al. (2006) and Strader et al. (2006) found that, in giant ellipticals such as M87, NGC4649 and NGC7094, luminous blue GCs (i.e. metal-poor GCs) reveal a trend of having redder colors, such that more massive GCs are more red (metal-rich). This trend is referred to as a ‘blue tilt’ (also see Brodie & Strader 2006). This ‘blue tilt’ was interpreted as a result of self-enrichment (Strader et al. 2006). Strader et al. (2006) speculatively suggested that these GCs once possessed dark matter halos. Spitler et al. (2006) subsequently found that this ‘blue tilt’ is also true in the Sombrero spiral galaxy (NGC4594) and may extend to less luminous GCs with a somewhat shallower slope that was derived by Harris et al. (2006) and Strader et al. (2006). As Spitler et al. (2006) pointed out that, the Sombrero provides the first example of this trend in a spiral galaxy and in a galaxy found in a low-density galaxy environment. However, in these ACS studies, the metal-rich (red) GCs did not show this corresponding trend (also see Bekki et al. 2007). Based on high-resolution cosmological simulation with globular clusters, Bekki et al. (2007) investigated formation processes and physical properties of globular cluster system in galaxies, and found that, luminous metal-poor clusters would emerge a correlation between luminosity and metallicity if they originated from nuclei of low-mass galaxies at high z . In fact, in the simulations of Bekki et al. (2007), the ‘simulated blue tilts’ emerge from the assumption that luminous metal-poor clusters originate from stellar galactic nuclei of the more massive nucleated galaxies with a luminosity-metallicity relation. So, it is evident that, in Bekki et al. (2007), galaxies which experienced more accretion/merging events of nu-

cleated low-mass galaxies are more likely to show a blue tilt (see details from Bekki et al. 2007).

3. SUMMARY

In this paper we present spatial and metal abundance properties of 95 M81 globular clusters, which are collected by Ma et al. (2005). This cluster sample includes nearly half of the M81 total globular cluster population, is the largest one comparing to the total globular clusters of the host galaxy beyond the Local Group. Our conclusions are as follows:

1. The metal-rich clusters did not demonstrate a centrally concentrated spatial distribution as ones in M31, and metal-poor clusters tend to be less spatially concentrated. Most of metal-rich clusters distribute at projected radii of 4-8 kpc. We can conclude that most of the metal-rich clusters in our sample are not associated with a bulge cluster system of M81; they may associate with a thick disk in M81 as indicated by Schroder et al. (2002).

2. The globular clusters in M81 have a small radial metallicity gradient like M31 and our Galaxy, suggesting that some dissipation occurred during the formation of the globular cluster system.

3. There is not obvious trend of metallicity with luminosity in M81 globular clusters.

We are indebted to the referee for his/her thoughtful comments and insightful suggestions that improved this paper greatly. This work has been supported by the Chinese National Natural Science Foundation Nos 10473012, 10573020, 10633020, 10673012 and 10603006; and by National Basic Research Program of China (973 Program) No. 2007CB815403.

REFERENCES

- Armandroff, T. E. 1989, *AJ*, 97, 375
 Ashman, K. A., Bird, C. M., & Zepf, S. E. 1994, *AJ*, 108, 2348
 Barmby, P., Huchra, J., Brodie, J., Forbes, D., Schroder, L., & Grillmair, C. 2000, *AJ*, 119, 727
 Barmby, P., & Huchra, J. 2001, *AJ*, 122, 2458
 Bekki, K., Yahagi, H., & Forbes, D. A. 2007, *MNRAS*, 377, 215
 Brodie, J. P., & Huchra, J. P. 1990, *ApJ*, 362, 503
 Brodie, J. P., & Huchra, J. P. 1991, *ApJ*, 379, 157
 Brodie, J., & Strader, J. 2006, *ARA&A*, 44, 193
 Bruzual, G., & Charlot, S. 1996, unpublished
 Chandar, R., Ford, H. C., & Tsvetanov, Z. 2001, *AJ*, 122, 1330
 Chandar, R., Whitmore, B., & Lee, M. G. 2004, *ApJ*, 611, 220
 Côté, P. 1999, *AJ*, 118, 406
 Eggen O. J., Lynden-Bell D., & Sandage A. R. 1962, *ApJ*, 136, 748
 Elson, R. A., & Walterbos, R. A. M. 1988, *ApJ*, 333, 594
 Forbes, D. A., Brodie, J. P., & Larsen, S. S. 2001, *ApJ*, 556, L83
 Freedman, W. L., Wilson, C. D., & Madore, B. F. 1994, *ApJ*, 427, 628
 Frenk, C. S., & White, S. D. M. 1982, *MNRAS*, 198, 173
 Gebhardt, K., & Kissler-Patig, M. 1999, *AJ*, 118, 1526
 Harris, W. E., Whitmore, B. C., Karakla D., Okoń, W., Baum, W. A., Hanes, D. A., & Kavelaars, J. J. 2006, *ApJ*, 636, 90
 Huchra J., Stauffer J., & van Speybroeck L. 1982, *ApJ*, 259, L57
 Huchra J. P., Brodie J. P., & Kent, S. M. 1991, *ApJ*, 370, 495
 Kong, X., et al. 2000, *AJ*, 119, 2745
 Kundu, A., & Whitmore, B. C. 2001, *AJ*, 121, 2950
 Larsen, S. S., et al. 2001, *AJ*, 121, 2974
 Ma, J., et al. 2005, *PASP*, 117, 256
 Ma, J., et al. 2006, *PASP*, 118, 98
 Minniti, D. 1995, *AJ*, 109, 1663
 Parmentier, G., & Gilmore, G. 2001, *A&A*, 378, 97
 Parmentier, G., Jehin, E., Magain, P., Neuforge, C., Noels, A., & Thoul, A. A. 1999, *A&A*, 352, 138
 Peng, E. W., et al. 2006, *ApJ*, 639, 95
 Perelmuter, J. M., Brodie, J. P., & Huchra, J. 1995, *AJ*, 110, 620
 Perrett, K. M., et al. 2002, *AJ*, 123, 2490
 Perelmuter, J. M., & Racine, R. 1995, *AJ*, 109, 1055
 Reed, B. C., Hesser, J. E., & Shawl, S. J. 1988, *PASP*, 100, 545
 Schroder, L. L., Brodie, J. P., Kissler-Patig, M., Huchra, J. P., & Phillips, A. C. 2002, *AJ*, 123, 2473
 Searle, L., & Zinn, R. 1978, *ApJ*, 225, 357
 Sharov, A. S. 1988, *Soviet Astron. Lett.*, 14, 339
 Spitler, L. R., Larsen, S. S., Strader, J., Brodie, J. P., Forbes, D. A., & Beasley, M. A. 2006, *AJ*, 132, 1593
 Strader, J., Brodie, J. P., Spitler, L., & Beasley, M. A. 2006, *AJ*, 132, 2333
 van den Bergh, S. 1969, *ApJS*, 19, 145
 West, M. J., Côté, P., Marzke, R. O., & Jordan, A. 2004, *Nature*, 427, 31
 Zepf, S. E., & Ashman, K. A. 1993, *MNRAS*, 264, 611
 Zinn, R. 1985, *ApJ*, 293, 424

TABLE 1
GLOBULAR CLUSTER SAMPLE AND PROPERTIES

ID ^a	[Fe/H]	Distance from M81 center (kpc)	ID ^a	[Fe/H]	Distance from M81 center (kpc)
Id30244	-1.53 ± 0.072	24.9	CFT5	-0.87 ± 0.070	8.5
Is40083	-1.29 ± 0.80	39.4	CFT6	-1.40 ± 0.084	8.4
Is40165	-1.57 ± 0.43	20.7	CFT8	-0.90 ± 0.060	7.3
Is40181	-0.76 ± 0.072	19.9	CFT15	-1.81 ± 0.314	9.9
Is50037	-2.34 ± 0.83	15.7	CFT16	-1.53 ± 0.360	8.8
Is50225	-0.04 ± 0.59	7.7	CFT20	-1.46 ± 0.205	8.0
Is50233	-1.23 ± 0.072	6.5	CFT21	-1.50 ± 0.263	9.3
Is50286	-1.45 ± 0.072	8.1	CFT22	-0.70 ± 0.253	7.3
Id50357	-0.33 ± 0.072	11.1	CFT28	-1.24 ± 0.393	7.4
Is50394	-2.17 ± 0.072	10.0	CFT30	-1.09 ± 0.128	9.3
Id50401	-0.72 ± 0.072	5.7	CFT31	-0.54 ± 0.502	8.9
Id50415	-1.90 ± 0.71	4.6	CFT32	-0.08 ± 0.205	9.2
Id50696	-1.86 ± 0.50	3.5	CFT34	-1.25 ± 0.174	9.2
Id50785	-1.58 ± 0.072	6.1	CFT37	-1.80 ± 0.031	3.2
Is50861	-1.38 ± 0.072	6.0	CFT38	-1.44 ± 0.029	3.2
Is50886	-1.79 ± 0.87	6.9	CFT39	-1.29 ± 0.022	3.4
Id50960	-1.79 ± 0.64	9.4	CFT41	-1.59 ± 0.022	3.1
Is51027	-2.06 ± 0.072	9.5	CFT42	-1.52 ± 0.034	2.6
Is60045	-1.03 ± 0.97	20.9	CFT43	-1.62 ± 0.138	2.6
Id70319	-1.00 ± 0.072	16.3	CFT44	-1.61 ± 0.123	4.1
Id70349	-1.19 ± 0.072	18.3	CFT45	-1.63 ± 0.043	5.1
Is80172	-0.77 ± 0.68	20.7	CFT46	-1.66 ± 0.051	4.7
Is90103	-2.23 ± 0.99	37.5	CFT49	-1.67 ± 0.191	4.6
SBKHP1	-1.207 ± 0.369	4.9	CFT51	-0.35 ± 0.084	5.1
SBKHP2	-0.707 ± 0.167	4.5	CFT53	-1.81 ± 0.058	6.5
SBKHP3	-0.211 ± 0.193	3.2	CFT56	-1.63 ± 0.034	3.8
SBKHP4	-0.407 ± 0.088	2.9	CFT58	0.21 ± 0.343	3.7
SBKHP5	-1.086 ± 0.091	2.2	CFT62	-1.11 ± 0.017	4.6
SBKHP6	-1.493 ± 0.206	1.7	CFT63	-1.69 ± 0.628	4.2
SBKHP7	-0.955 ± 0.098	1.6	CFT65	-1.87 ± 0.080	2.7
SBKHP8	-0.698 ± 0.058	2.4	CFT66	-1.85 ± 0.077	4.7
SBKHP9	-1.212 ± 0.133	2.7	CFT67	-1.31 ± 0.092	3.1
SBKHP10	-1.322 ± 0.356	4.0	CFT68	-1.62 ± 0.060	4.9
SBKHP11	-1.114 ± 0.409	4.8	CFT74	-1.72 ± 0.060	5.9
SBKHP12	-1.06 ± 0.072	5.1	CFT75	-1.64 ± 0.046	5.6
SBKHP13	-1.055 ± 0.062	7.6	CFT76	-1.87 ± 0.046	5.9
SBKHP14	-1.107 ± 0.074	5.9	CFT80	-1.79 ± 0.152	6.8
SBKHP15	-1.014 ± 0.713	8.2	CFT83	-1.63 ± 0.282	10.0
SBKHP16	-0.674 ± 0.044	7.1	CFT85	-1.61 ± 0.203	9.0
CFT87	-0.66 ± 0.087	5.9	FT106	-0.93 ± 0.147	4.7
CFT90	-0.51 ± 1.733	5.6	FT108	-1.00 ± 0.123	3.8
CFT96	0.95 ± 0.792	6.2	FT109	-0.50 ± 0.234	3.1
CFT97	-1.22 ± 0.056	6.4	FT110	-1.29 ± 0.215	2.6
FT101	-1.44 ± 0.386	5.0	FT111	-1.14 ± 0.150	4.7
FT102	0.01 ± 0.659	5.9	FT112	-1.79 ± 0.256	4.5
FT103	-1.65 ± 0.263	5.8	FT113	-0.68 ± 0.140	7.7
FT104	-1.30 ± 0.082	4.8	FT114	-1.73 ± 0.159	3.4
FT105	-1.02 ± 0.075	4.0			

This figure "f1.jpg" is available in "jpg" format from:

<http://arxiv.org/ps/0708.4083v1>